

Natural Convection Heat Transfer in Horizontal Concentric Annulus between Outer Cylinder and Inner Flat Tube

Waleed Mohammed Abed

Instructor

University of Anbar /Engineering College -Mechanical Engineering Dept.

Received on : 11/5/2010

Amer Jameel Shareef

Asst. Instructor

Ahmed Ali Najeeb

Asst. Instructor

Accepted on : 8/12/2010

Abstract.

Natural convection heat transfer in two-dimensional region formed by constant heat flux horizontal flat tube concentrically located in cooled horizontal cylinder studied numerically. The model solved using the FLUENT CFD package. The numerical simulations covered a range of hydraulic radius ratio (5, 7.5, and 10) at orientation angles from (0° up to 90°).

The results showed that the average Nusselt number increases with hydraulic radius ratio, orientation angles and Rayleigh number. As well as enhancement ratio for Nusselt number at orientation angle 90° and hydraulic radius ratio 7.5 equal 24.87%. Both the fluid flow and heat transfer characteristics for different cases are illustrated velocity vectors and temperature contours that obtained from the CFD code. The results for the average Nusselt numbers are compared with previous works and show good agreement.

Key words: Natural Convection, Horizontal Annulus, Flat Tube, Aspect Ratio, Orientation Angle.

1. Introduction.

Natural convection in an annulus concentric cylinder has been extensively investigated due to the variety of technical applications and practicality such as heat transfer in heat exchanger device, solar collectors, nuclear reactor, cooling of electrical and electronic components, thermal storage system, electrical transmission cables, etc. Among the problems related to natural convection, many researchers focused their investigation on the heat transfer and fluid flow behavior from differentially heated walls in a square or cubic cavity. However, the heat transfer mechanism and fluid flow behavior in a concentric annulus cylinder are strongly depended on the aspect ratio which is defined as a ratio of the diameter of the outer to the inner cylinder. The temperature different between the heated inner cylinder and cold outer cylinder contributes the density gradient and circulate the fluid in the annulus. The next important dimensionless parameters are the Rayleigh and Prandtl numbers, which affect the heat transfer mechanism, the flow pattern and the stability of the transitions of flow in the system [1,2].

One of the first, well documented studies of heat transfer in horizontal annular enclosures was presented by Beckmann [3]. He performed experimental measurements for three different gases, air; H_2 and CO_2 , for the ranges of aspect ratio and Gr_{Di} where $1.1875 \leq Do/Di \leq 8.1$ and $3.4 \times 10^3 \leq Gr_{Di} \leq 1.5 \times 10^7$. Kuehn and Goldstein [4] studied natural convection in annular cavities filled with pressurized nitrogen over a Rayleigh number range of $2.2 \times 10^2 \leq Ra \leq 7.7 \times 10^7$ and for radii ratio 2.6. The results showed that the flow is unstable in the plume region for $Ra = 2 \times 10^5$ and that the flow becomes turbulent as Ra is increased. Also, they reported that over the inner cylinder the flow is turbulent and that under the inner cylinder the flow is laminar. Comparatively, fewer publications were noticed for natural convection in non-circular domain, Rayleigh number range of $7 \times 10^2 \leq Ra \leq 10^4$ and for radii ratio 1.32, Lee and Lee [5] attempted to formulate the free convection problem in terms of

elliptical coordinates for the symmetrical cases of oblate and prolate elliptical annuli and have performed experiments for this geometry.

The problem of free convection heat transfer from horizontal elliptic cylinder placed with its major axis vertical in a fluid of infinite extent is investigated by Bader and Shamsher [6]. Their problem was solved for Rayleigh number varies from 10 to 10^3 , $Pr=0.7$, and the cylinder axis ratio (minor/major) varies from 0.1 to 0.964. Bader [7] studied the effect of elliptic cylinder orientation. The cylinder orientation varies horizontal to vertical major axis while the axis ratio ranges from (0.4 to 0.98) at two Rayleigh numbers of 10^3 and 10^4 .

Teertstra et al. [8] developed an analytical model for natural convection in the two dimensional region formed by an isothermal. The model is comprised of a combination of three solutions, the diffusive limit, the laminar boundary layer limit, and the transition flow limit, and is applicable to a wide range of aspect ratios and inner and outer boundary shapes. The model and data are in good agreement, with an average RMS difference of 6% for the circular annulus and less than 9% for the other geometries. Djeddar et al. [9] expressed the Boussinesq equations of the laminar thermal and natural convection, in the case of permanent and flow, in an annular space between two concentric elliptic cylinders. They use a new calculation code with the finite volumes with the primitive functions (velocity-pressure formulation) and the elliptic coordinates system. The Prandtl number is constant at 0.7 and internal elliptic tube ($e_1 = 0.999, 0.9, \text{ and } 0.83$) the eccentricity of the external elliptic tube is maintained constant ($e_2 = 0.75$) with varying the Grashof number ($Gr = 10^3, 10^4, 10^5$ and 2×10^5). The authors examined effect of the geometry of the interior elliptic cylinder on the results.

Eid [10] studied natural convection heat transfer in elliptic annuli with different aspect ratios experimentally and numerically. Four test specimens having elliptic annuli cross sections with different aspect ratios of 0.25 to 1 and an annulus diameter ratio of 2 were tested experimentally. The model was solved numerically using the FLUENT CFD package. The results show that the rotation of the elliptic annuli with small aspect ratio by a right angle whenever the specimens are horizontal or inclined improves the free convective heat transfer characteristics. The numerical predictions show that the annulus diameter ratio has more significant effect on the results rather than the orientation mode.

Sakr et al. [11] investigated experimental and numerical of natural convection heat transfer in horizontal elliptic annuli. Experiments were carried out for Rayleigh number ranges from 1.12×10^7 up to 4.92×10^7 , the elliptic tube orientation angle, θ , varies from 0° to 90° and the hydraulic radius ratio of 6.4. These experiments were carried out for axis ratio of elliptic tube (minor/major= b/c) of 1:3. The numerical simulation for the problem is carried out by using commercial CFD code. The numerical simulations covered a range of elliptic tube axis ratio from 0.1 to 0.98 and for hydraulic radius ratio from 1.5 to 6.4. Both the average and local Nusselt number from the experimental results are compared with those obtained from the CFD code. Both the fluid flow and heat transfer characteristics for different operating and geometric conditions are illustrated velocity vectors and isotherms contours that obtained from the CFD code.

Padilla and Silveira-Neto [12] are performed large-eddy simulations of transition to turbulence in a horizontal annular cavity. Solutions for Prandtl number of (0.707), hydraulic radius ratio of (2) and Rayleigh number 4.6×10^4 up to 7.5×10^5 are obtained. The influences of transitional and turbulent flows on local and mean Nusselt number are also investigated.

Nada [13] investigated experimental natural convection heat transfer in horizontal and inclined annular fluid layers. The annulus inner surface is maintained at high temperature by applying heat flux to the inner tube while the annulus outer surface is maintained at low temperature by circulating cooling water at high mass flow rate around the outer tube. The experiments were carried out at a wide range of Rayleigh number (5×10^4 up to 5×10^5) for

different annulus gap widths ($L/D_0= 0.23, 0.3, \text{ and } 0.37$) and different inclination of the annulus ($\theta= 0^\circ, 30^\circ \text{ and } 60^\circ$). The results showed that:

- (1) Increasing the annulus gap width strongly increases the heat transfer rate.
- (2) The heat transfer rate slightly decreases with increasing the inclination of the annulus from the horizontal.

Azmir and Azwadi [14] presented numerical study of flow behavior from a heated concentric annulus cylinder at various Rayleigh number ($2.38 \times 10^3 \leq Ra \leq 1.02 \times 10^5$), Prandtl number (0.716, 0.717 and 0.718) and aspect ratio of the outer and inner cylinders (2.6, 3.6, 4.6 and 5). The finite different lattice Boltzmann method (FDLBM) numerical scheme is proposed to improve the computational efficiency and numerical stability of the conventional method. Current investigation concluded that the FDLBM is an efficient approach for the current problem in hand and good agreement with the published papers in literature solution. The above survey, of horizontal annulus studies and data as summarized in **table (1)**.

In the present work, the present contribution presents a simulation of the problem as a mathematical model which was solved numerically using the FLUENT-CFD package. The present problem to investigate the effect of Rayleigh number, aspect ratio (hydraulic radius ratio), and different orientation angle of the heated flat tube placed in an isothermal cooled circular cylinder on the natural convection heat transfer.

2. Mathematical model.

Consider an annular space ranging from a flat tube placed at the center of a circular cylinder filled with air. The internal wall of the annular space (flat tube surface) heater under constant heat flux q_H , and the external wall of the annular space (circular cylinder surface) keep isothermally at temperature T_c . The inner flat tube is allowed to be inclined to the horizontal axis by an orientation angle; θ . The physical model of the present problem is illustrated in **Fig. (1-a)**. The natural convection heat transfer between outer cylinder and inner flat tube results in a buoyancy-driven flow in a vertical $r-\theta$ plane. The space coordinates are r , measured from the center of the cylinder and, θ , measured anti-clockwise from the downward vertical symmetry line. The two-dimensional governing equations were summarized as follows under the following assumptions, [15, 16]:

- a) Steady state.
- b) Two dimensional heat transfer.
- c) The laminar flow.
- d) The fluid is incompressible.
- e) Constant properties except change in density, according to Boussinesq approximation.
- f) The viscous dissipation is negligible.

The present problem is governed equations of continuity, momentum and energy. These equations can be written in the form:

Continuity equation:

$$\frac{\partial V_r}{\partial r} + \frac{V_r}{r} + \frac{1}{r} \frac{\partial V_\theta}{\partial \theta} = 0 \quad (1)$$

r-momentum equation:

$$\rho \left(V_r \frac{\partial V_r}{\partial r} + \frac{V_\theta}{r} \frac{\partial V_r}{\partial \theta} - \frac{V_\theta^2}{r} \right) = -\frac{\partial p}{\partial r} + \mu \left[\frac{\partial}{\partial r} \left(\frac{1}{r} \frac{\partial}{\partial r} (V_r r) \right) + \frac{1}{r^2} \left(\frac{\partial^2 V_r}{\partial \theta^2} \right) - \frac{2}{r^2} \frac{\partial V_\theta}{\partial \theta} \right] + F_r \quad (2)$$

θ -momentum equation:

$$\rho \left(V_r \frac{\partial V_\theta}{\partial r} + \frac{V_\theta}{r} \frac{\partial V_\theta}{\partial \theta} - \frac{V_r V_\theta}{r} \right) = -\frac{1}{r} \frac{\partial p}{\partial \theta} + \mu \left[\frac{\partial}{\partial r} \left(\frac{1}{r} \frac{\partial}{\partial r} (V_\theta r) \right) + \frac{1}{r^2} \left(\frac{\partial^2 V_\theta}{\partial \theta^2} \right) + \frac{2}{r^2} \frac{\partial V_r}{\partial \theta} \right] + F_\theta \quad (3)$$

Energy equation:

$$\left(V_r \frac{\partial T}{\partial r} + \frac{V_\theta}{r} \frac{\partial T}{\partial \theta} \right) = \alpha \left[\left(\frac{1}{r} \frac{\partial}{\partial r} (r) \frac{\partial T}{\partial r} \right) + \frac{1}{r^2} \left(\frac{\partial^2 T}{\partial \theta^2} \right) \right] \quad (4)$$

The buoyancy forces in r and θ directions are written as:

$$F_r = \rho g \beta (T - T_c) \sin \theta$$

$$F_\theta = \rho g \beta (T - T_c) \cos \theta$$

The boundary conditions

At the surface of the flat tube, ($r = Ri$; $0 \leq \theta \leq 2\pi$), $V_r = V_\theta = 0$, $\frac{\partial T}{\partial r} = const.$

At the surface of the outer cylinder, ($r = Ro$; $0 \leq \theta \leq 2\pi$), $V_r = V_\theta = 0$, $T = T_c$

3. Numerical method.

The governing equations were solved using FLUENT-CFD code; version 6.2 is employed for all numerical simulations [17]. Gambit, Version 2.2.30, is used for the development of the computational grid. **Fig. (1-b)** shows the computational grid. The computational domain resulted from the subtraction of the flat tube section from the circular cylinder section. The grid is made up of triangular elements to improve the quality of the numerical prediction near the curved surfaces. The continuity is satisfied using a semi-implicit method for pressure linked equations, which is referred to as the SIMPLE procedure. To reduce numerical errors, second order upwind discrimination schemes are used in the calculations. Each computational iteration is solved implicitly. The convergence of the computational solution is determined on scaled residuals for the continuity, energy equations and for many of the predicted variables. The total residual for a given variable is based on the imbalance in an equation for conservation of that variable summed over all computational cells. Less than 1000 iterations are generally needed for convergence.

4. Results and discussions.

Figs. (2, 3, 4) show the variation of the average Nusselt number with Rayleigh number for different hydraulic radius ratio (5, 7.5, and 10) at orientation angles, ($0^\circ, 45^\circ$, and 90°). The Nusselt number increases with increasing Rayleigh number. This is because the Nusselt number depends on the heat transfer rate. In addition, figures show the effect of hydraulic radius ratio on the Nusselt number. It can be seen clearly from the figures that the Nusselt numbers at higher hydraulic radius ratio are higher than those at lower ones. The increase of hydraulic radius ratio causes higher fluid re-circulation and higher swirl flow air in the annular space due to the gradient in density, and consequently, the Nusselt number increase with increasing hydraulic radius ratio. It is also found from these figures. the enhancement in Nusselt Number at hydraulic radius ratio.

($Ro/Ri=5$), orientation angle from 0° to 45° (19.8%), as from $\theta=0^\circ$ to $\theta=90^\circ$ (24.3%). While, enhancement in Nusselt Number at ($Ro/Ri=7.5$) from $\theta=0^\circ$ to $\theta=45^\circ$ (19.4%) and from $\theta=0^\circ$ to $\theta=90^\circ$ (24.87%). ($Ro/Ri=10$) from $\theta=0^\circ$ to $\theta=45^\circ$ (18.98%), from $\theta=0^\circ$ to $\theta=90^\circ$ (24.22%).

The effect of the orientation angle on the flow and thermal fields contours are illustrated in **Figs. (5, 6)**. It is observed that both the velocity vectors and temperature (isotherms) contours are symmetric about the vertical axis of the flat tube for orientation angle 90° . A thermal plume above the flat tube is observed for all inclination angles. Also, it is observed that as the orientation angle increases the temperature gradient decreases, indicating that more cooling for the flat tube surface. The thermal plume size increase with heat flux at all orientation different angles.

Figs. (7, 8, 9) show the variation of the average Nusselt number with Rayleigh number for orientation angles, ($0^\circ, 45^\circ$, and 90°) at different hydraulic radius ratio (5, 7.5, and 10). The average Nusselt number increases with increasing orientation angles at the same value of Rayleigh number. In the other word, the maximum heat transfer rate occurs at 90° orientation angle. **Fig. (10)** show the velocity vector and temperature contours for $Ro/Ri=5$ to 10 at orientation angle of 45° and $q_H=4.0W/m^2$.

Figs. (11, 12) show the variation of the average Nusselt number with orientation angles for different hydraulic radius ratio (5, 7.5, and 10) at heat flux 10, $800W/m^2$ respectively. The average Nusselt number increases with increasing orientation angles. In the other word, the maximum heat transfer rate occurs at hydraulic radius ratio 10. In other wise, it is observed that from the these **Figs.** the rapid increase in the average Nusselt number in the range of orientation angles (0° to 45°) after this orientation angles range the increase in the average Nusselt number forward to fixed. The increase of the hydraulic radius ratio leads to increase in the average Nusselt number for different orientation angles based on the equivalent hydraulic radius of the flat tube. This is may be attributed to the longer annuli (path) of the air fluid layer with higher velocity at higher hydraulic radius ratio. The best enhancement in Nusselt Number at $\theta=90^\circ$ and $Ro/Ri=7.5$ which is (24.87%).

As well as the previous work Sakr et al. [11], see **Fig. (13)** this figure shows that the present results are good agreement with the previous work.

5. Conclusions.

Natural convection heat transfer between outer cylinder and inner flat tube was investigated numerically using the FLUENT CFD package.

1. The average Nusselt number increases with the increase of the flat tube orientation angle.
2. Both the velocity vector and temperature contours are symmetric about the major axis of the flat tube only at an angles of orientation of 0° , and 90° , which corresponding to maximum rate of heat transfer condition.
3. The average Nusselt number increases with the increase of Rayleigh number.
4. The average Nusselt number increases with the increase of the hydraulic radius ratio.

6. References.

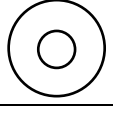
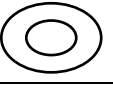


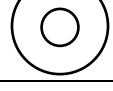

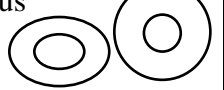
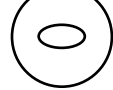
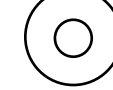


- [1] Jaluria Y., " Natural Convection Heat and Mass Transfer – Volume 5 ", William Clowes (Beccles) Limited, Beccles and London, First Edition, 1980.
- [2] Kays W. M. and Crawford M. E., " Convective Heat and Mass Transfer ", McGraw-Hill, Inc., Third Edition, 1993.
- [3] Teertstra P. and Yovanovich M.M., " Comprehensive review of natural convection in horizontal circular annuli ", 7th AIAA/ASME Joint Thermophysics and heat transfer conference, Albuquerque, NM, June 15-18, 1998.
- [4] Kuehn T.H. and Goldstein R.J., " An Experimental and Theoretical Study of Natural Convection Heat Transfer in Concentric and Eccentric Horizontal Cylindrical Annuli " ASME J. of Heat Transfer, Vol. 100, pp.635-640, 1978.

- [5] Lee J.H. and Lee T.S., " Natural Convection in the Annuli between Horizontal Confocal Elliptical Cylinders" Int. J. Heat and Mass Transfer, Vol. 24, pp. 1739-1742, 1981.
- [6] Bader H.M. and Shamsheer K., "Free Convection from an Elliptic Cylinder with Major Axis Vertical" Int. J. Heat and Mass Transfer, Vol. 36, No. 14, pp. 3593-3602, 1993.
- [7] Bader, H.M., " Laminar Natural Convection from an Elliptic Tube with Different Orientations" ASME J. of Heat Transfer, Vol. 119, pp.709-718, 1997.
- [8] Teertstra P., Yovanovich M. M., Culham J. R.," Analytical Modeling of Natural Convection in Horizontal Annuli" Published by the American Institute of Aeronautics and Astronautics (AIAA- 0959), 2005.
- [9] Djezzar M., Chaker A., and Daguinet M.," Numerical Study of Bidimensional Steady Natural Convection in a Space Annulus Between Two Elliptic Confocal Ducts Influence of the Internal Eccentricity ", Rev. Energ. Ren. J., Vol. 8, pp. 63-72, 2005.
- [10] Eid E. I.," Natural Convection Heat Transfer in Elliptic Annuli with Different Aspect Ratios", Alexandria Engineering Journal, Vol. 44, No. 2, pp. 203-215, 2005.
- [11] Sakr R.Y., Berbish N.S., Abd-Alziz A.A. and Hanafi A.S.," Experimental and Numerical Investigation of Natural Convection Heat Transfer in horizontal Elliptic Annuli " Journal of Applied Sciences Research, Vol.4, No. 2, pp.138-155, 2008.
- [12] Padilla E. L. M. and Silveira-Neto A.," Large-eddy Simulations of Transition to Turbulence in a Horizontal Annular Cavity ", Int. J. of Heat and Mass Transfer, Vol. 51, pp. 3656-3668, 2008.
- [13] Nada S. A.," Experimental Investigation of Natural Convection Heat Transfer in Horizontal and Inclined Annular Fluid Layers", Int. J. of Heat and Mass Transfer, Vol. 44, No. 8, pp. 929-936, 2008.
- [14] Azmir O. Shahrul and Azwadi C. S. Nor," UTOPIA Finite Different Lattice Boltzmann Method for Simulation Natural Convection Heat Transfer from a Heated Concentric Annulus Cylinder" European Journal of Scientific Research -ISSN 1450-216X, Vol.38, No.1, pp.63-71, 2009.
- [15] Patankar S.V., "Numerical Heat Transfer and Fluid Flow ", McGraw-Hill Book Company, New York, 1980.
- [16] Versteeg H.K. and Malalasekera W.," An Introduction to Computation Fluid Dynamics, The Finite Volume Method ", John Wiley, Sons Inc., 605 Third Avenue, New York, USA, 1995.
- [17] Fluent," FLUENT-CFD user's guide ", Lebanon, Fluent Inc., USA, 2000.

7. Nomenclature.

F	Force (N)	T	Temperature (°C)
g	Gravity acceleration (m/s ²)	V	Velocity (m/s)
h	Heat transfer coefficient (W/m ² .°C)		Greek Samples
k	Thermal conductivity (W/m. °C)	α	Thermal diffusivity (m ² /s)
L	Length (m)	β	Volume coefficient of expansion (K ⁻¹)
Nu	Nusselt number	θ	Orientation angle (°)
P	Perimeter (m)	μ	Dynamic viscosity (N.s/m ²)
Pr	Prandtl number	ρ	Density (kg/m ³)
p	Pressure (Pa.)		Subscript
Q	Heat transfer rate (W)	c	cold
q _H	Heat flux (W/m ²)	h	hot
R	Radius (m)	o	outer
Ra	Rayleigh number	r	radial coordinate (m)
Ro/Ri	Hydraulic radius ratio	θ	tangential direction

Table 1: Review of horizontal annulus studies and data.

Authors	Test	Range of independent parameters	Geometry
Kuehn and Goldstein [4]	Experimental and Theoretical	$2.2 \times 10^2 \leq Ra \leq 7.7 \times 10^7$, $Po/Pi = 2.6$	Horizontal circular annulus 
Lee and Lee [5]	Experimental	$7 \times 10^2 \leq Ra \leq 10^4$, $Po/Pi = 1.32$	Elliptic cylinder 
Bader and Shamsher [6]	Experimental	$10 \leq Ra \leq 10^3$, $Pr = 0.7$, (minor/major) varies from 0.1 to 0.964	Elliptic annulus 
Bader [7]	Experimental	$10^3 \leq Ra \leq 10^4$, $Pr = 0.7$, (minor/major) varies from 0.4 to 0.98	Elliptic annulus 
Teertstra et al. [8]	Numerical	$Po/Pi = 2.12$ to 6.37	Circular annulus 
Djezzar et al. [9]	Numerical	$Pr = 0.7$, ($e_1 = 0.999, 0.9$, and 0.83) ($e_2 = 0.75$) ($Gr = 10^3, 10^4, 10^5$ and 2×10^5)	Elliptic cylinder 
Eid [10]	Experimental and Numerical	$1 \times 10^5 \leq Ra \leq 500 \times 10^5$ $Po/Pi = 0.25$ to 1	Elliptic and circular annulus 
Sakr et al. [11]	Experimental and Numerical	$1.12 \times 10^7 \leq Ra \leq 4.92 \times 10^7$, annulus inclination ($\theta, 0^\circ$ to 90°), $Po/Pi = 6.4$	Horizontal elliptic tube 
Padilla and Silveira-Neto [12]	Numerical	$Pr = 0.707$, $Po/Pi = 2$ $4.6 \times 10^4 \leq Ra \leq 7.5 \times 10^5$	Horizontal circular annulus 
Nada [13]	Experimental	$5 \times 10^4 \leq Ra \leq 5 \times 10^5$ ($L/D_o = 0.23, 0.3$, and 0.37) annulus inclination ($\theta = 0^\circ, 30^\circ$ and 60°).	Horizontal circular annulus 
Azmir and Azwadi [14]	Numerical	$2.38 \times 10^3 \leq Ra \leq 1.02 \times 10^5$, $Pr = 0.716, 0.717, 0.718$ $Po/Pi = 2.6, 3.6, 4.6$ and 5	Horizontal circular annulus 

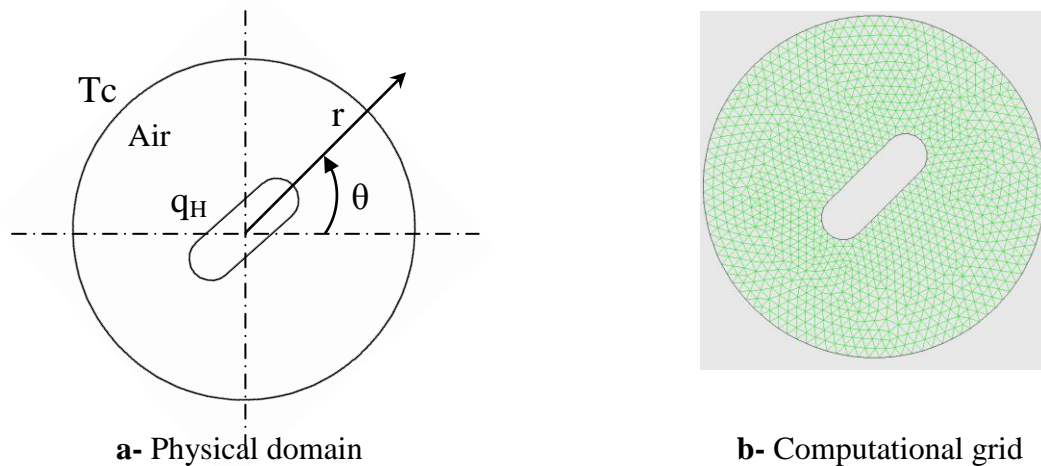


Fig. (1): Physical domain and computational grid.

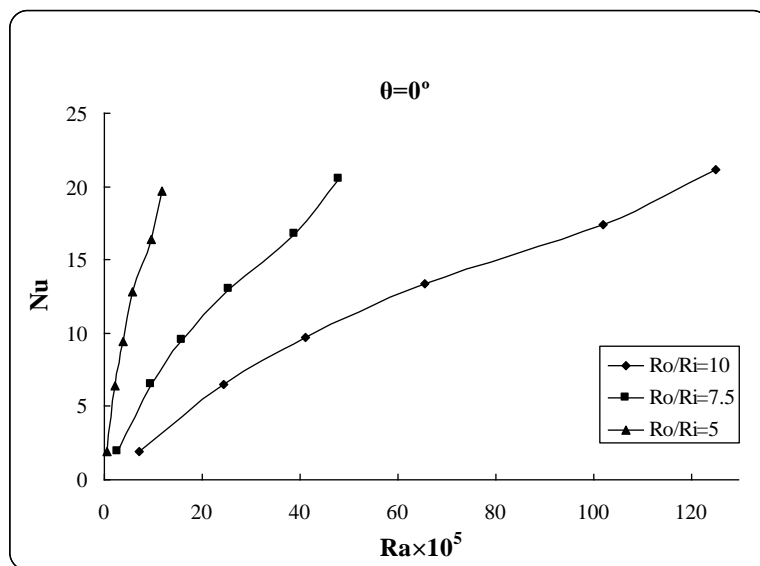


Fig. (2): The variation of average (Nu) with (Ra) at orientation angle, 0° , for different (Ro/Ri).

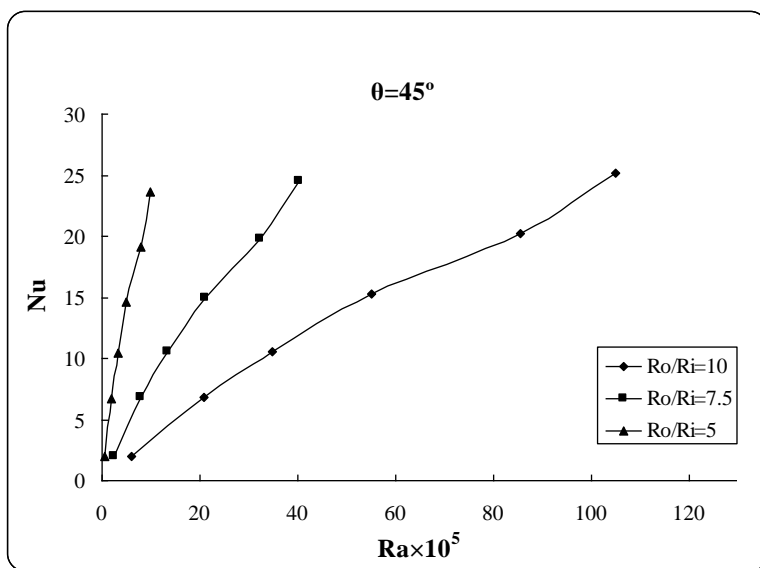


Fig. (3): The variation of average (Nu) with (Ra) at orientation angle, 45° , for different (Ro/Ri).

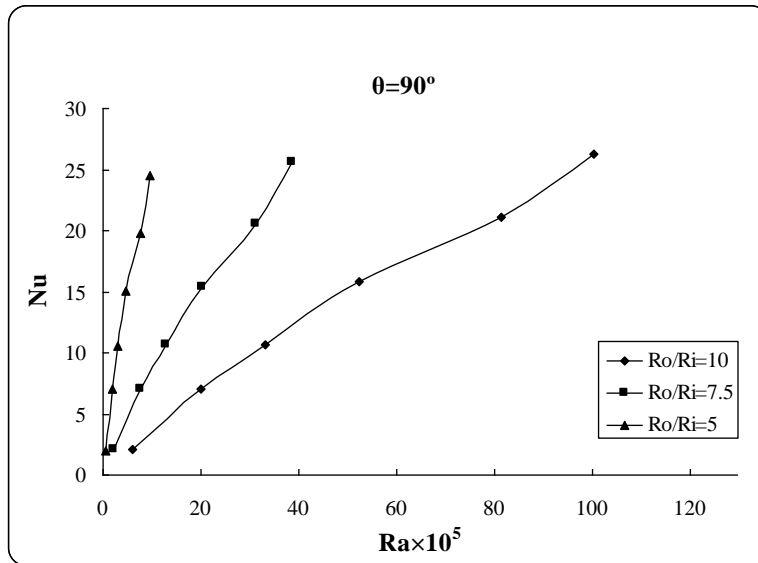


Fig. (4): The variation of average (Nu) with (Ra) at orientation angle, 90°, for different (Ro/Ri).

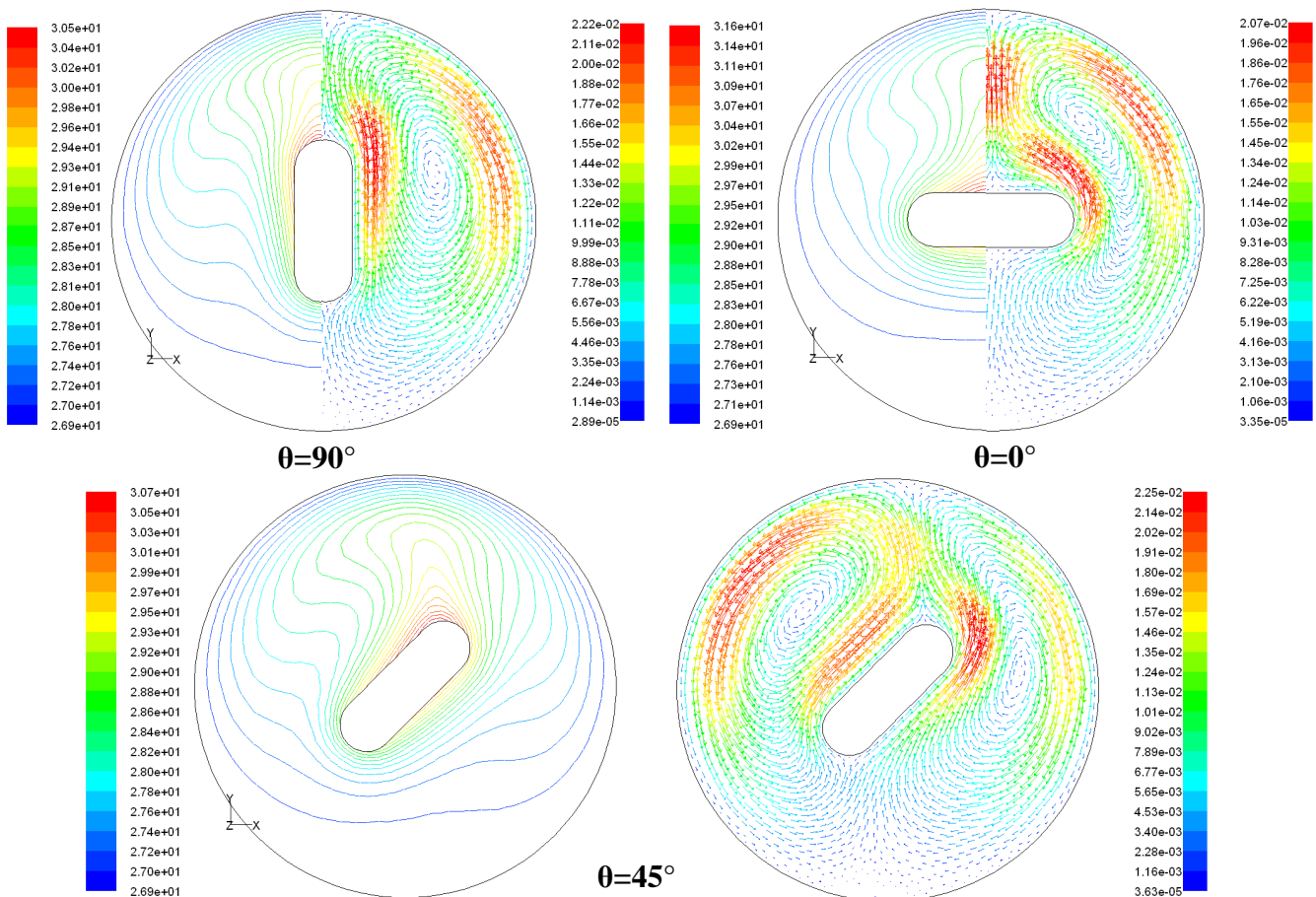


Fig. (5): Velocity vectors and temperature contours for different orientation angle $Ro/Ri=5$, $q_H=10W/m^2$.

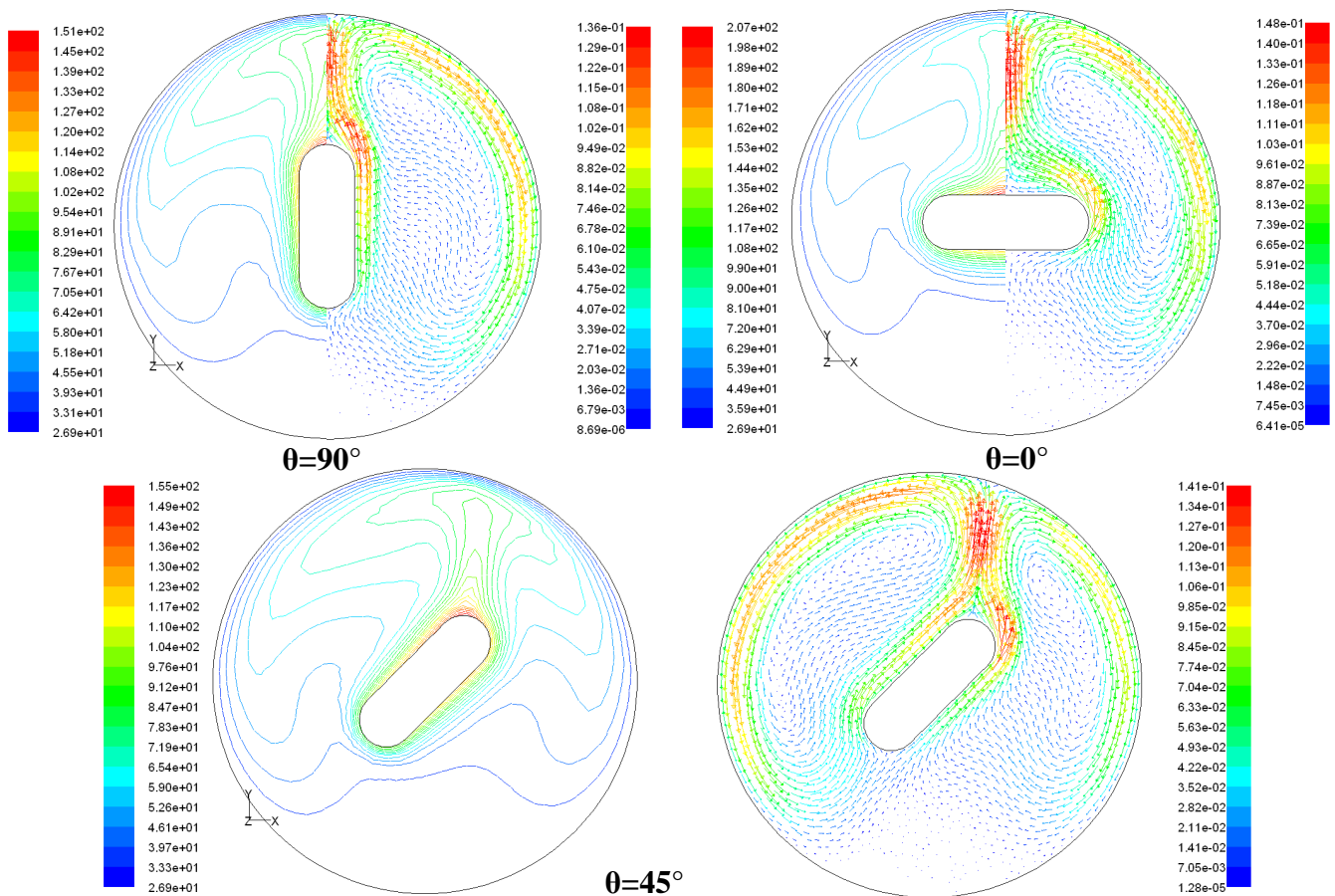


Fig. (6): Velocity vectors and temperature contours for different orientation angle $Ro/Ri=5$, $q_H=800W/m^2$.

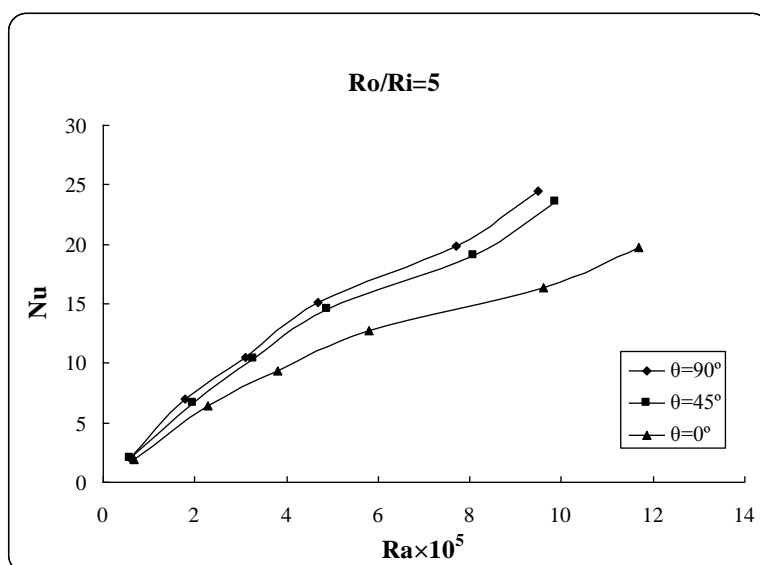


Fig. (7): The variation of the average (Nu) with the (Ra) for different orientation angle at ($Ro/Ri =5$).

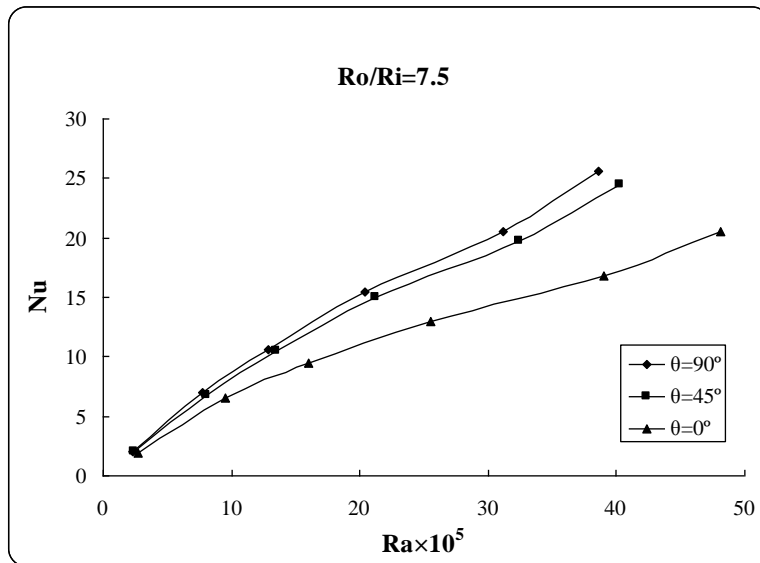


Fig. (8): The variation of the average (Nu) with the (Ra) for different orientation angle at (Ro/Ri =7.5).

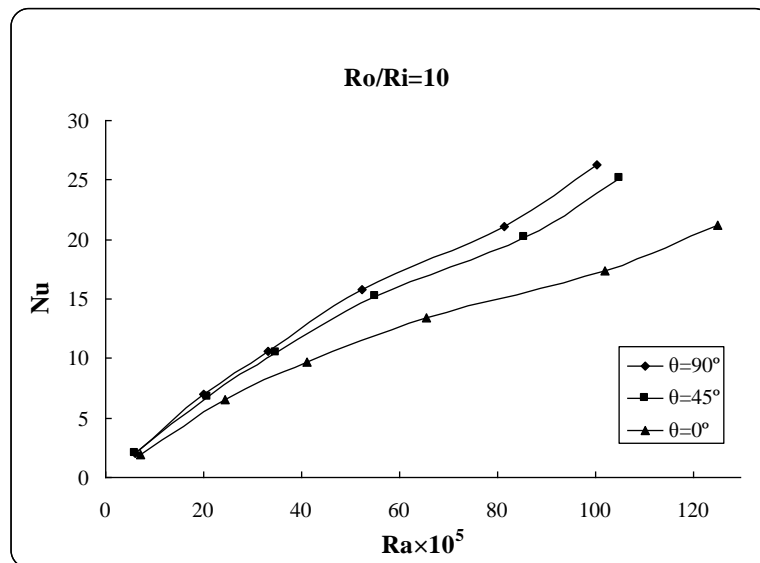


Fig. (9): The variation of the average (Nu) with the (Ra) for different orientation angle at (Ro/Ri =10).

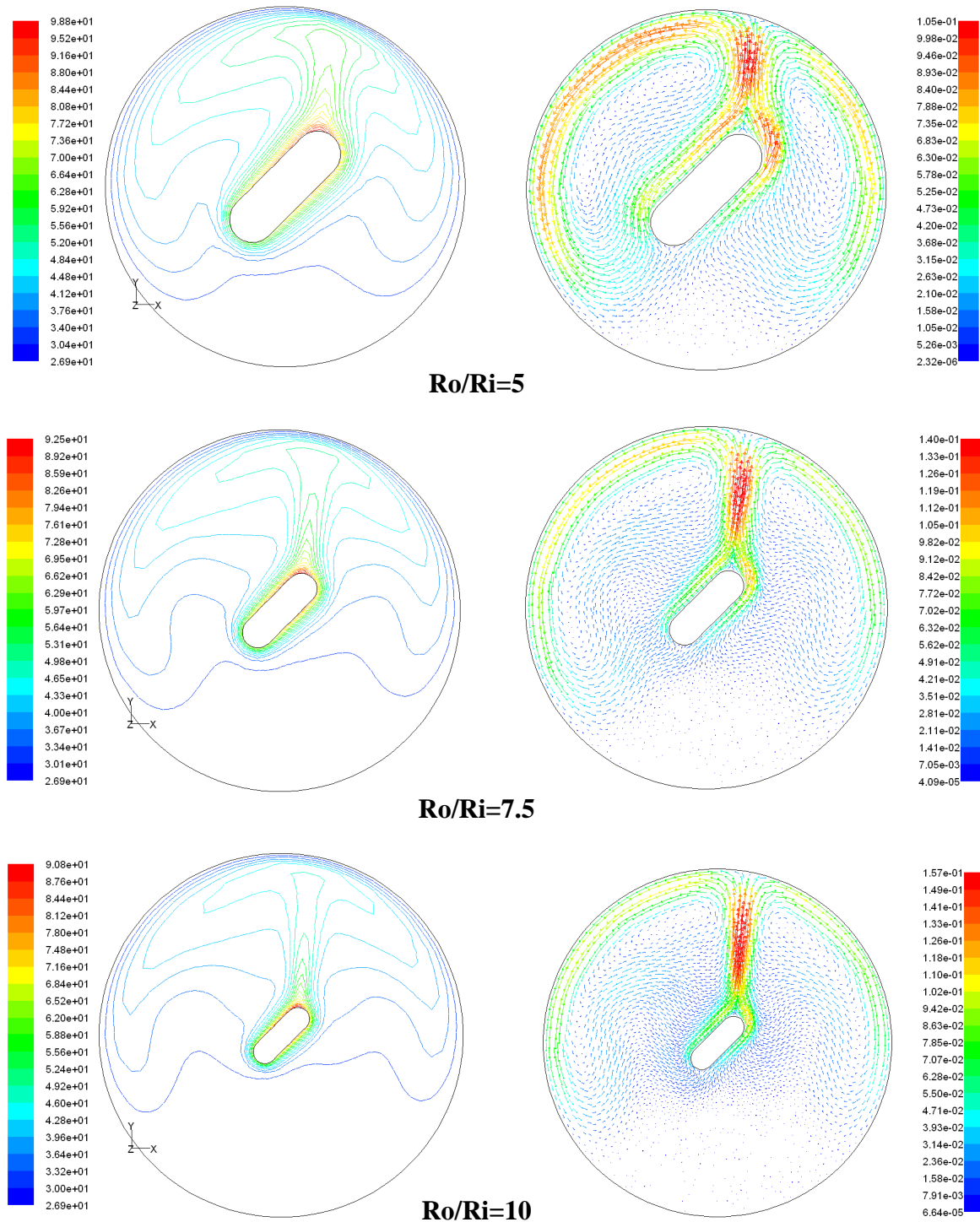


Fig. (10): Velocity vectors and temperature contours for $\theta=45^\circ$, $q_H=400\text{W/m}^2$.

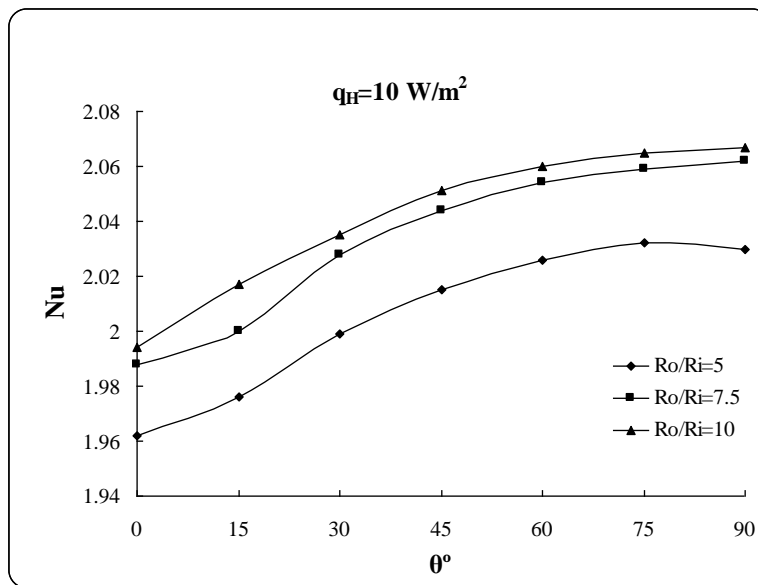


Fig. (11): The variation of the Nu with θ for different Ro/Ri at $q_H=10\text{W/m}^2$.

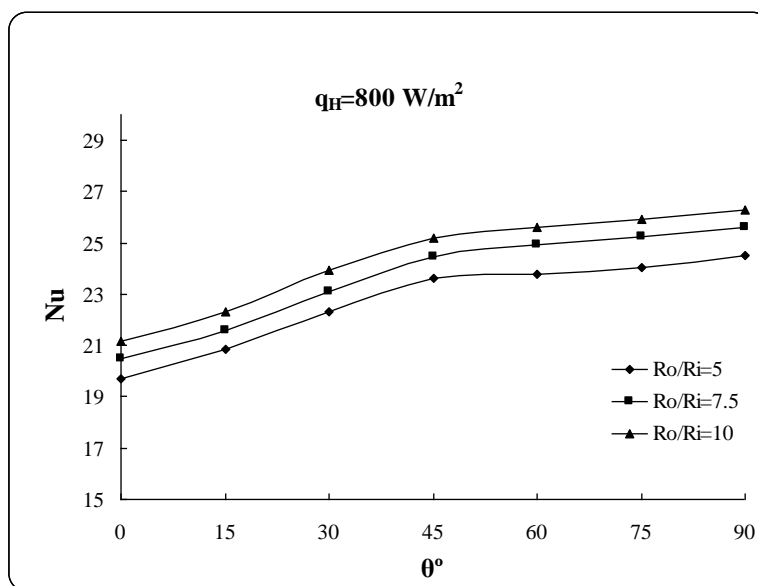


Fig. (12): The variation of the Nu with θ for different Ro/Ri at $q_H=800\text{W/m}^2$.

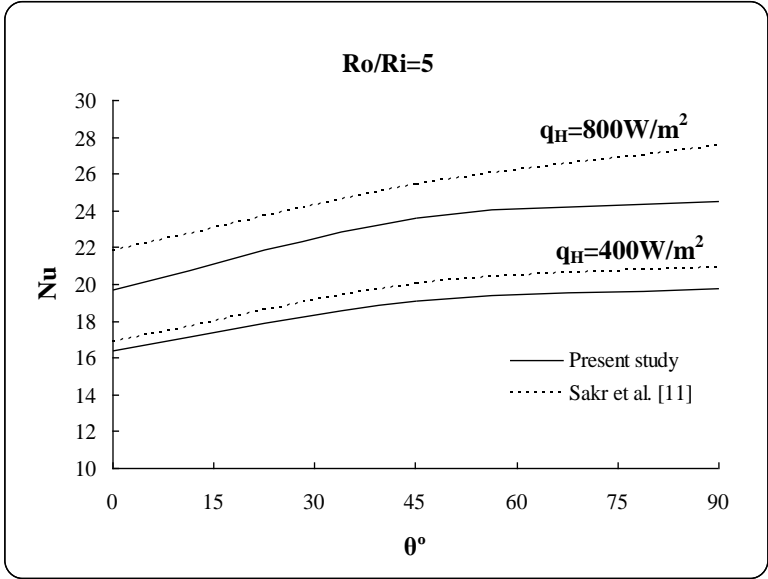


Fig. (13): Comparison between the present numerical predictions with the previous work.

انتقال الحرارة بالحمل الحر في أنبوب حلقي أفقي متحد المركز بين اسطوانة خارجية وأنبوب مسطح داخلي

احمد علي نجيب
مدرس مساعد / كلية الهندسة
جامعة الانبار

عامر جميل شريف
مدرس مساعد / كلية الهندسة
جامعة الانبار

وليد محمد عبد
مدرس / كلية الهندسة
جامعة الانبار

الخلاصة.

تضمن البحث دراسة عددية لانتقال الحرارة بالحمل الحر في منطقة ثنائية الأبعاد لأنبوب حلقي أفقي متحد المركز بين أنبوب مسطح عند فيض حراري ثابت داخل اسطوانة مبردة. تم حل النموذج الرياضي باستخدام برنامج معد خصيصا للحل العددي (FLUENT CFD package)، تناولت المحاكاة العددية مدى نسبة أنصاف الأقطار الهيدروليكية (5، 7.5، 10) عند زوايا توجيه من 0° الى 90° . بينت النتائج بأن متوسط عدد نسلت يزداد بزيادة كل من نسبة نصف القطر الهيدروليكي، زوايا توجيه الأنبوب المستوي وعدد رايلي، وجد أن أفضل نسبة تحسن لقيم عدد نسلت عند زاوية توجيه 90° و نسبة أنصاف الأقطار الهيدروليكية (7.5) هي (24.87%). مثلت خصائص جريان المائع وانتقال الحرارة لحالات مختلفة بمخططات درجة الحرارة و متجه السرعة. عند مقارنة نتائج البحث الحالي مع البحوث السابقة تم الحصول على توافق جيد.